

© Team of authors, 2024 / © Коллектив авторов, 2024

3.1.10. Neurosurgery / 3.1.10. Нейрохирургия

Anatomical evaluation of parasellar middle cranial fossa triangles

Bollavaram Pullanna¹, Ramakrishna Avadhani¹, Viveka S.², Anoop Shastry³

¹Yenepoya University, Mangalore, Karnataka, India

²Healiosmed Academy, Bangalore, Karnataka, India

³Shivananda Shastry, Super speciality hospital, shikaripura, Shivamogga, Karnataka, India

Contacts: Bollavaram Pullanna – vaas111766@gmail.com

Анатомическая оценка параселлярных треугольников средней черепной ямки

Боллаварам Пулланна¹, Рамакришна Авадхани¹, Вивека С.², Ануп Шастри³

¹Университет Енепойя, Мангалур, Карнатака, Индия

²Академия Хеалиосмед, Бангалор, Карнатака, Индия

³Специализированная больница имени Шивананды Шастри, Шикарипура, Шивамогга, Карнатака, Индия

Контакты: Боллаварам Пулланна – vaas111766@gmail.com

解剖学评估颅底中部副鞍区三角

Bollavaram Pullanna¹, Ramakrishna Avadhani¹, Viveka S.², Anoop Shastry³

¹Yenepoya University, Mangalore, Karnataka, India

²Healiosmed Academy, Bangalore, Karnataka, India

³Shivananda Shastry, Super speciality hospital, shikaripura, Shivamogga, Karnataka, India.

通讯作者: Bollavaram Pullanna – vaas111766@gmail.com

Introduction: various surgical approaches to parasellar region have been developed, necessitating a thorough understanding of the microsurgical anatomy.

The objectives of this study were to delineate the borders of parasellar middle cranial fossa triangles and to morphometrically evaluate of these triangles.

Methodology: in a cross-sectional observational study design, conducted in Department of Anatomy from May 2021 to August 2022, borders, morphometry and contents of parasellar middle cranial fossa triangles were delineated in fifteen cranial fossa specimens.

Results: the medial border of clinoid triangle formed by optic nerve was the shortest with average length of 7.64 mm (\pm 0.59 mm) and lateral border formed by oculomotor nerve was the longest with average measurement of 14.5 mm (\pm 1.46 mm). The medial border of oculomotor triangle formed by interclinoid dural fold had average length of 9.05 mm (\pm 1.07 mm) and lateral border formed by anterior petroclinoid dural fold had average measurement of 14.38 mm (\pm 2.61 mm). The oculomotor nerve forming the medial limit of supratrochlear triangle measured 10.81 mm (\pm 1.25 mm) and lateral trochlear nerve border measured 14.94 (\pm 1.08 mm).

Conclusion: morphometric measurements of parasellar middle cranial fossa triangles, namely, clinoid triangle, oculomotor triangle, supratrochlear and infratrochlear triangle are presented.

Keywords: parasellar region; clinoid triangle, oculomotor triangle, supratrochlear and infratrochlear triangle, morphometry

Conflicts of interest. The authors have no conflicts of interest to declare.

Funding. There was no funding for this study

For citation: Bollavaram Pullanna, Ramakrishna Avadhani, Viveka S., Anoop Shastry. Anatomical evaluation of parasellar middle cranial fossa triangles. Head and neck. Russian Journal. 2024;12(1):34–41

Doi: 10.25792/HN.2024.12.1.34-41

The authors are responsible for the originality of the data presented and the possibility of publishing illustrative material – tables, drawings, photographs of patients.

Введение: Разнообразие хирургических подходов к параселлярной области требует глубокого понимания микрохирургической анатомии.

Целью данного исследования было определение границ параселлярных треугольников средней черепной ямки и морфометрическая оценка этих треугольников.

Материалы и методы: в ходе перекрестного наблюдательного исследования, проведенного на кафедре анатомии с мая 2021 по август 2022 г., на пятнадцати образцах черепной ямки были определены границы, морфометрические параметры и содержимое параселлярных треугольников средней черепной ямки.

Результаты: медиальная граница клиновидного треугольника, образованная зрительным нервом, была самой короткой, составляя в среднем 7,64 мм ($\pm 0,59$ мм) в длину, а латеральная граница, образованная глазодвигательным нервом, была самой длинной и достигала в среднем 14,5 мм ($\pm 1,46$ мм). Средняя длина медиальной границы глазодвигательного треугольника, образованной межклиновидной складкой твердой мозговой оболочки, составила 9,05 мм ($\pm 1,07$ мм), а латеральной границы, образованной передней петроклиновидной складкой твердой мозговой оболочки, - 14,38 мм ($\pm 2,61$ мм). Глазодвигательный нерв, формирующий медиальную границу супратрохлеарного треугольника, имел длину 10,81 мм ($\pm 1,25$ мм), а латеральная граница по блоковому нерву - 14,94 мм ($\pm 1,08$ мм).

Заключение: представлены морфометрические параметры параселлярных треугольников средней черепной ямки: клиновидного треугольника, глазодвигательного треугольника, надблокового и подблокового треугольников.

Ключевые слова: параселлярная область; клиновидный треугольник, глазодвигательный треугольник, надблоковый и подблоковый треугольники, морфометрия

Конфликт интересов. Авторы заявляют об отсутствии конфликта интересов.

Финансирование. Работа выполнена без спонсорской поддержки.

Для цитирования. Боллаварам Пулланна, Рамакришна Авадхани, Вивека С., Аноуп Шастри. Анатомическая оценка параселлярных треугольников средней черепной ямки. *Head and neck. Голова и шея. Российский журнал.* 2024;12(1):34–41

Doi: 10.25792/HN.2024.12.1.34-41

Авторы несут ответственность за оригинальность представленных данных и возможность публикации иллюстративного материала – таблиц, рисунков, фотографий пациентов.

介绍: 各种手术方法已被开发用于治疗蝶鞍区, 这就需要对显微外科解剖有深入的了解。本研究的目标是划定蝶鞍区中颅窝三角形的边界, 并对这些三角形进行形态测量评估。

方法: 在2021年5月至2022年8月期间, 在解剖学系进行的横断面观察性研究设计中, 对十五个颅窝标本的蝶鞍区中颅窝三角形的边界、形态测量和内容进行了划分。

结果: 由视神经形成的翼结节三角形的内侧边界是最短的, 平均长度为7.64毫米 (± 0.59 毫米), 由动眼神经形成的外侧边界是最长的, 平均长度为14.5毫米 (± 1.46 毫米)。由间翼结节硬脑膜襞形成的动眼神经三角形的内侧边界平均长度为9.05毫米 (± 1.07 毫米), 由前岩翼结节硬脑膜襞形成的外侧边界平均长度为14.38毫米 (± 2.61 毫米)。构成眶上三角形内限的动眼神经测量为10.81毫米 (± 1.25 毫米), 外侧滑车神经边界测量为14.94毫米 (± 1.08 毫米)。

结论: 蝶鞍区中颅窝三角形, 即翼结节三角形、动眼神经三角形、眶上和眶下三角形的形态测量值在本文中被提出。

关键词: 蝶鞍区域; 岩锥三角、动眼神经三角、眶上和眶下三角, 形态测量

利益冲突: 作者声明没有任何利益冲突。

资金来源: 本研究没有资金支持。

引用本文: **Bollavaram Pullanna, Ramakrishna Avadhani, Viveka S., Anoop Shastry. Anatomical evaluation of parasellar middle cranial fossa triangles. Head and neck. Russian Journal.** 2024;12(1):34–41

Doi: 10.25792/HN.2024.12.1.34-41

作者负责所呈现数据的原创性以及出版插图材料——表格、图画、患者照片的可能性。

Introduction

Various surgical approaches to middle cranial fossa especially in parasellar region have been developed in the recent past, necessitating a thorough understanding of the microsurgical anatomy [1]. In addition, endoscopic endonasal surgical techniques are frequently used to explore the medial cavernous sinus region [2]. As the endoscopic view and transcranial view of the parasellar

region differ significantly, it is prudent to be well-versed with the identified dissecting corridors and to know the safe area of manoeuvring in this region [3]. Especially so in the skull base, as the operating space is often too minimal and any deviations from the operating protocol proves catastrophic. However, normative values of the measurements of the structures and spaces related the parasellar region are missing. The identified parasellar middle cranial fossa triangles are clinoidal (anteromedial or Dolenc) triangle,

oculomotor (medial or Hakuba's) triangle, supratrochlear triangle and infratrochlear (Parkinson's) triangle [2].

Clinoidal (anteromedial or Dolenc) triangle is bordered by the optic nerve, oculomotor nerve and tentorial edge (and the dura extending between the dural entry point of the third cranial nerve and the optic nerve) [4]. Clinoidal segment of internal carotid artery (ICA) and the anterior clinoid process (ACP) are located here. Anterior clinoid process has three roots: anterior root (attached to the planum medial to falciform ligament), posterior root (optic strut) and third root (attachment of anterior clinoid process to the lesser wing of sphenoid) [5]. Oculomotor (medial or Hakuba's) triangle is located in relation to middle cranial fossa bounded by anteriorly by anterior petroclinoid dural fold, posteriorly by posterior petroclinoid dural fold, and medially by the interclinoid dural fold [6]. Its contents are the oculomotor nerve and horizontal segment of ICA. Also, in this space the origin of meningohypophyseal trunk, the initial intracavernous course of the abducens nerve, and the interclinoid ligament can be visualized. This triangle is important during oculomotor nerve exposure [7]. Oculomotor nerve courses just below the dura of the anterior clinoid process (lower margin) [8]. Oculomotor nerve has its own cistern (oculomotor cistern) up to the tip of the anterior clinoid process [8]. To expose the clinoid segment of ICA, anterior clinoid process needs to be removed. Upper dural ring defines the superior limit of clinoid segment of ICA. Upper dural ring extends medially from upper surface of anterior clinoid process. Lower dural ring, also called Perneckzy's ring, defines the inferior limit of the clinoid segment of ICA [9]. Lower dural ring extends from the lower surface of anterior clinoid process. It separates the clinoid process from the upper surface of the oculomotor nerve. This dural sheath continues medially as the carotid-oculomotor membrane (COM) [10]. COM covers the carotid artery. Ophthalmic artery arises just above the clinoid segment. Opening the clinoid and oculomotor triangles with removal of anterior clinoid process up to the optic strut exposes COM [10]. Supratrochlear triangle (or paramedian triangle) is located between the lower aspect of oculomotor nerve (medial border) and upper aspect of trochlear nerve (lateral border). The dura between these two nerves (3rd and 4th) forms the third boundary [11]. It has meningohypophyseal trunk. Frequently inferolateral trunk and medial loop of ICA are located within this triangle. In the posterior part of the cavernous sinus, trochlear nerve is inferior to oculomotor nerve. In the anterior part, it turns upwards and at the level of optic strut, it becomes the most superior part of the cavernous sinus [12]. Trochlear nerve is always superior to the maxillary nerve. As the presence of inferolateral trunk and medial loop of ICA are not constant, evaluating the contents of the supratrochlear triangle provides anatomical details about the cavernous segment of the trochlear nerve [13].

Infratrochlear triangle (Parkinson's triangle) is bounded by inferior margin of trochlear nerve (medial border), superior margin of ophthalmic nerve (lateral border) and tentorial edge (base). It has cavernous part of ICA and abducent nerve [14]. Dissection in this triangle exposes the abducent nerve [15]. Parkinson described this triangle for direct entry to the cavernous sinus [16, 17]. Few authors have called inferior trochlear triangle as lateral triangle [4, 18]. Dissecting this triangle is important in exposing the trochlear nerve.

With this background, the study was designed with the objectives delineate the borders of parasellar middle cranial fossa triangles and to morphometrically evaluate of these triangles.

Methodology

In a cross-sectional observational study design, conducted in Department of Anatomy from May 2021 to August 2022, borders,

morphometry and contents of parasellar middle cranial fossa triangles were delineated in fifteen cranial fossa specimens. Institutional ethics committee and scientific review board approved the protocol before starting the study (letter number YEC-1/2021/049).

Cadaveric evaluation

After removal of calvaria, the occipital bone and squama of temporal bones were cut up to the transverse sinus and attachment of tentorium cerebelli. The falx cerebri attachment to the crista galli was severed, and carefully reflected outwards cutting any bridging veins connecting the superficial cortical veins and superior sagittal sinus.

Cranial nerves in their order were cut under vision away from the skull base, towards the brain to retain the part of the nerves entering the skull base foramen. The pituitary stalk was also cut similarly. The internal carotid artery was cut after ophthalmic artery branching (in the intracerebral segment). The temporal lobe was carefully delivered out of the temporal fossa and a linear incision was taken along the attached margin of the tentorium cerebelli. Tentorium is slid backwards cutting any bridging veins from inferior anastomotic vein of Labbe.

The brainstem is blunt cut with the finger as far down as possible in relation to the clivus. The brain was removed intact. The cranial fossa thus exposed was inspected.

Inclusion criteria: all fresh cadavers used for routine undergraduate dissection during the study duration where brain removal was undertaken were included in the study. The skull base specimens available in the Department of Anatomy with no damages to the cavernous sinus and related structures, with intact dura over the anterior, middle and posterior cranial fossa were included in the study.

Exclusion criteria: specimen with cavernous sinus structures previously dissected, with no dural covering over the anterior, middle and posterior cranial fossa were excluded. Specimens with no identifiable intracranial segments of oculomotor, trochlear, trigeminal and abducens nerves were also excluded.

The specimen thus prepared were examined under 3X to 20X magnification using a surgical microscope. The triangles considered in the study were evaluated. A square shaped incision was made in the dura from lesser wing of sphenoid to the planum sphenoidale. This exposes the anterior clinoid process, optic canal and sphenoid edge. Bony canal of the optic canal was removed and anterior clinoid process was drilled. This exposes the clinoidal triangle. The borders of this triangles were noted. Dura over the middle cranial fossa was meticulously removed leaving all the cranial nerves in situ. Structures related to the lateral wall of cavernous sinus was noted. Every effort will be made to avoid any changes in the anatomical relationships of the related structures at this step. All the structures were photographed. At this stage, limits and contents of supratrochlear and infratrochlear were noted.

The measurements were taken with digital scale. Right and left sides were compared. Area was calculated as $\sqrt{p(p-a)(p-b)(p-c)}$ where p is half of the perimeter, or $p = (a+b+c)/2$ and a, b and c were length of boundaries [19]. If the area of the triangle cannot be calculated with this formula as the case when the sum of two side lengths does not exceed the length of the third side, those area calculations are excluded from measure of central tendency. The consistency in shape and size were noted between the specimens.

Measurements and statistical analysis

Clinoid triangle: medial border is measured as length of the optic nerve within the optic canal. Initially, the intra-canalicular part of the optic nerve is marked, bony covering of the optic canal removed



Figure 1: Boundaries of clinoid triangle, also showing the clinoid part of internal carotid artery (ICA).

Рис. 1. Границы клиновидного треугольника, также показан клиновидный сегмент внутренней сонной артерии (ВСА)

and measurements of intracanalicular part of the optic nerves were taken. The lateral border was measured from oculomotor nerve from dural entry point up to the entry point of superior orbital fissure. Base is the tentorial edge extending between the dural entry point of oculomotor nerve and optic nerve.

Oculomotor triangle: anterior clinoid process, posterior clinoid process and petrous apex is identified as most prominent palpable bony projections under the dural folds. Lateral border of oculomotor triangle is measured from the anterior clinoid process tip to the petrous apex and correspond to anterior petroclinoid ligament. Medial border of this triangle measured from posterior clinoid process to the petrous apex and correspond to posterior petroclinoid ligament. Base of the triangle representing the interclinoid dural fold was measured from anterior clinoid process to posterior clinoid process.

Supratrochlear triangle: medial border and lateral borders are measured as distances from dural entry points of oculomotor nerve and trochlear nerve up to the superior orbital fissure. Base was measured between the dural entry points of oculomotor and trochlear nerves.

Infracrochlear triangle: medial border and lateral borders are measured as distances from dural entry points of trochlear nerve

and ophthalmic nerve up to the superior orbital fissure. Base was measured between the dural entry points of trochlear and ophthalmic nerves.

To take the measurements, surgical microscope, Almicrosterio zoom microscope (Micro Measures & Instruments, Haryana, India) was used. This three-dimensional zoom trinocular microscope has a high point wide field eye pieces 10x and 15x, parfocal zoom objectives of 1x to 5x provides continuous variable magnification from 10x to 150x depending upon the eye pieces and supplementary lens used, having well designed pole stand, extension pillar, 360 revolving zoom trinocular head, 6 volts 21 watts incident spot light illuminator with light control transformer. Each specimen was placed at 5 cm from the objective of the microscope and images are obtained. Along with every measurement, a measuring scale of length 10mm was also be kept for standardization. Each measurement was taken twice and by two observers to avoid inter and intra-observational bias. Average values of these recordings were considered for analysis. All measurements were expressed in millimetres.

Results

Out of fifteen cadavers 14 were male and one was female.

Clinoid triangle: The measurements of clinoid triangle are tabulated in table 1. The medial border formed by optic nerve was the shortest with average length of 7.64 mm (± 0.59 mm) and lateral border formed by oculomotor nerve was the longest with average measurement of 14.5 mm (± 1.46 mm) (Figure 1). There was no statistically significant difference between right and left side of clinoid triangle. Clinoid segment of ICA was noted clearly after severing the anterior clinoid process (Figure 2 and Figure 3).

The morphometric measurements of anterior clinoid process are presented in Table 2. The measurements had no statistical difference between right and left side. The average length of clinoid part of internal carotid artery was 4.2 mm (± 0.41 mm), with maximum and minimum lengths being 4.75 mm and 3.33 mm. There was no statistical difference between right side measurements and left side measurements.

Oculomotor triangle: The measurements of oculomotor triangle are tabulated in table 2. The medial border formed by interclinoid

Table 1: tabulation of parameters observed in clinoid triangle (n=15)
Таблица 1: таблица параметров, наблюдаемых для клиновидного треугольника (n=15)

Clinoid triangle Клиновидный треугольник	Right side Справа				Left side Слева			
	Medial (mm) Медиальная (мм)	Lateral (mm) Латеральная (мм)	Base (mm) Основание (мм)	Area (mm ²) Площадь (мм ²)	Medial (mm) Медиальная (мм)	Lateral (mm) Латеральная (мм)	Base (mm) Основание (мм)	Area (mm ²) Площадь (мм ²)
Max Макс	8.89	16.30	10.68	32.08	8.72	16.54	10.27	36.21
Min Мин	7.00	11.91	7.10	12.11	7.12	13.01	6.58	22.84
Average Среднее	7.64	14.50	8.69	26.02	7.75	14.32	8.85	29.27
Standard deviation Стандартное отклонение	0.59	1.46	1.08	4.84	0.42	0.96	1.02	4.56
Upper CI Верхняя граница ДИ	7.94	15.24	9.24	28.47	7.96	14.81	9.37	31.58
Lower CI Нижняя граница ДИ	7.34	13.77	8.14	23.57	7.54	13.84	8.34	26.96
student t test t-критерий Стьюдента	0.56	0.69	0.68	0.07				



Figure 2: Clinoid part of Internal carotid artery (ICA) surface view after removing the clinoid process.

Рис. 2. Вид поверхности клиновидного сегмента внутренней сонной артерии (ВСА) после удаления наклоненного отростка

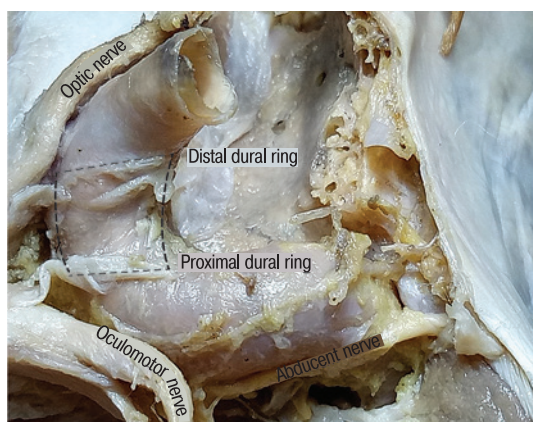


Figure 3: Clinoid part of Internal carotid artery (black dotted line) view after removing the clinoid process within the clinoid triangle

Рис. 3. Вид клиновидного сегмента внутренней сонной артерии (черная пунктирная линия) после удаления наклоненного отростка в пределах клиновидного треугольника

dural fold was the shortest with average length of 9.05 mm (± 1.07 mm) and lateral border formed by anterior petroclinoid dural fold was the longest with average measurement of 14.38 mm (± 2.61 mm) (Figure 4). There was no statistically significant difference between

right and left side of oculomotor triangle. The average length of the cavernous part of ICA within the triangle was 13.02 mm (± 1.53 mm) with maximum and minimum values being 15.88 mm and 10.91 mm respectively. The average distance of oculomotor nerve from apex of the triangle to dural entry point was 3.44 mm (± 0.86 mm) and from base to dural entry point was 6.23 mm (± 1.0 mm). The average thickness of the oculomotor nerve within the triangle was 1.6 mm (± 0.5 mm). Maximum thickness of 2.71 mm oculomotor nerve was observed on the left side in one of the specimens. There was no statistical difference between right and left side measurements.

Supratrochlear triangle: The measurements of supratrochlear triangle are tabulated in table 3. The oculomotor nerve forming the medial limit of the triangle measured 10.81 mm (± 1.25 mm) and lateral trochlear nerve border measured 14.94 (± 1.08 mm). There was no statistically significant difference between measurements of right and left side. In all the specimens, trochlear nerve was superior to maxillary nerve.

Infratrochlear triangle: The measurements of infratrochlear triangle are tabulated in table 4. The trochlear nerve forming the medial limit of the triangle measured 14.53 mm (± 1.18 mm) and ophthalmic division of trigeminal nerve forming the lateral border measured 12.83 (± 1.57 mm) (Figure 5). There was no statistically significant difference between measurements of right and left side.

Discussion

Paraclival, cavernous and paraclinoid segments of carotid artery and its relations are crucial for any skull base surgeries involving sellar region [20]. Though the endoscopic and transcranial view of the parasellar region differ significantly due to cavernous and clinoid segment of internal carotid artery hinders visualization of supratrochlear and infratrochlear triangles [12, 21] in this study, the morphometric analysis of these triangles (in addition to clinoid and oculomotor triangles) is considered through transcranial views in order to generate the normative values and to understand the variations in the contents of these triangles. Exposure of clinoid segment of internal carotid artery and optic nerve delineates the clinoid triangle. This gives access to superior cavernous sinus pathology extending to middle cranial fossa [22].

Table 2: tabulation of morphometric measurements of anterior clinoid process as noted within the clinoid triangle (n=15)
Таблица 2: таблица морфометрических параметров переднего наклоненного отростка, наблюдаемых внутри клиновидного треугольника (n=15)

Anterior clinoid process Передний наклоненный отросток	Right side Справа				Left side Слева			
	Medial (mm) Медиальная (мм)	Lateral (mm) Латеральная (мм)	Base (mm) Основание (мм)	Area (mm ²) Площадь (мм ²)	Medial (mm) Медиальная (мм)	Lateral (mm) Латеральная (мм)	Base (mm) Основание (мм)	Area (mm ²) Площадь (мм ²)
Max Макс	9.4	10.2	10.22	34.19	9.81	9.73	9.30	31.08
Min Мин	5.43	5.25	3.81	13.27	6.12	6.32	5.51	18.41
Average Среднее	7.08	7.43	7.31	22.42	7.53	8.28	7.62	25.48
Standard deviation Стандартное отклонение	1.04	1.31	1.49	6.18	1.02	1.10	1.00	3.77
Upper CI Верхняя граница ДИ	7.61	8.10	8.06	25.55	8.04	8.84	8.13	27.39
Lower CI Нижняя граница ДИ	6.55	6.77	6.55	19.30	7.01	7.73	7.11	23.57
student t test t-критерий Стьюдента	0.25	0.06	0.50	0.11				

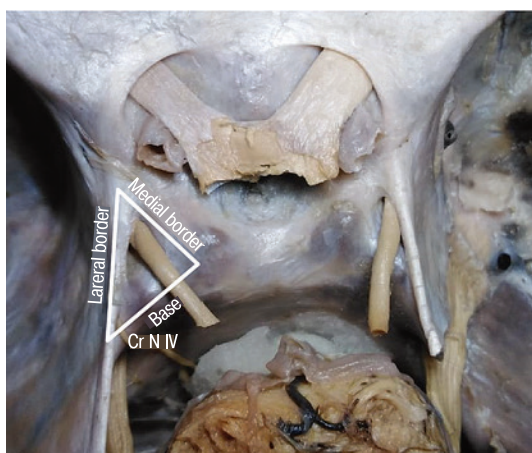


Figure 4: Boundaries of oculomotor triangle: medial, lateral and base. Cr N IV- trochlear nerve

Рис. 4. Границы глазодвигательного треугольника: медиальная, латеральная и основание. Cr N IV – блоковый нерв

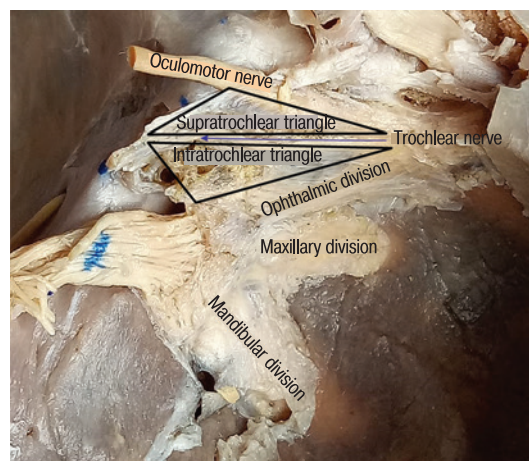


Figure 5: Dissection of supratrochlear and infratrochlear triangles, trochlear nerve is shown as blue line with arrow.

Рис. 5. Диссекция надблокового и подблокового треугольников, блоковый нерв показан синей линией со стрелкой

Table 3: tabulation of parameters observed in oculomotor triangle (n=15)

Таблица 3: таблица параметров, наблюдаемых для глазодвигательного треугольника (n=15)

Oculomotor triangle Глазодвигательный треугольник	Right side Справа				Left side Слева			
	Medial (mm) Медиальная (мм)	Lateral (mm) Латеральная (мм)	Base (mm) Основание (мм)	Area (mm ²) Площадь (мм ²)	Medial (mm) Медиальная (мм)	Lateral (mm) Латеральная (мм)	Base (mm) Основание (мм)	Area (mm ²) Площадь (мм ²)
Max Макс	11.21	17.78	15.63	74.50	11.93	17.11	13.63	66.55
Min Мин	7.77	9.17	8.05	32.80	8.05	11.04	8.20	32.86
Average Среднее	9.05	14.38	11.31	47.69	8.95	14.61	10.31	44.32
Standard deviation Стандартное отклонение	1.07	2.61	2.30	12.25	1.01	1.95	1.60	8.83
Upper CI Верхняя граница ДИ	9.59	15.70	12.48	53.89	9.46	15.60	11.12	48.79
Lower CI Нижняя граница ДИ	8.50	13.06	10.15	41.49	8.44	13.63	9.50	39.85
Student t test t-критерий Стьюдента	0.81	0.78	0.18	0.39				

Table 4: tabulation of parameters observed in supratrochlear triangle (n=15)

Таблица 4: таблица параметров, наблюдаемых для надблокового треугольника (n=15)

Supratrochlear triangle Надблоковый треугольник	Right side Справа				Left side Слева			
	Medial (mm) Медиальная (мм)	Lateral (mm) Латеральная (мм)	Base (mm) Основание (мм)	Area (mm ²) Площадь (мм ²)	Medial (mm) Медиальная (мм)	Lateral (mm) Латеральная (мм)	Base (mm) Основание (мм)	Area (mm ²) Площадь (мм ²)
Max Макс	12.48	17.28	7.08	29.33	13.77	16.86	8.54	30.32
Min Мин	8.69	13.71	4.08	7.88	8.51	5.92	3.87	12.38
Average Среднее	10.81	14.94	5.51	21.40	10.85	14.59	5.77	21.72
standard deviation Стандартное отклонение	1.25	1.08	1.10	6.60	1.25	2.65	1.32	5.11
upper CI Верхняя граница ДИ	11.44	15.48	6.07	24.74	11.49	15.93	6.44	24.31
Lower CI Нижняя граница ДИ	10.17	14.39	4.95	18.06	10.22	13.25	5.10	19.13
student t test t-критерий Стьюдента	0.92	0.65	0.57	0.88				

Table 5: tabulation of parameters observed in infratrochlear triangle (n=15)
Таблица 5: таблица параметров, наблюдаемых для подблокового треугольника (n=15)

Infratrochlear triangle Подблоковый треугольник	Right side Справа				Left side Слева			
	Borders Границы	Medial (mm) Медиальная (мм)	Lateral (mm) Латеральная (мм)	Base (mm) Основание (мм)	Area (mm ²) Площадь (мм ²)	Medial (mm) Медиальная (мм)	Lateral (mm) Латеральная (мм)	Base (mm) Основание (мм)
Max Макс	16.44	15.31	5.44	37.00	16.81	16.28	6.70	46.38
Min Мин	12.11	10.21	3.62	5.53	12.70	10.31	3.20	11.32
Average Среднее	14.53	12.83	4.53	24.67	14.51	13.02	4.75	25.76
standard deviation Стандартное отклонение	1.18	1.57	0.49	7.67	1.28	1.67	0.93	8.71
upper CI Верхняя граница ДИ	15.13	13.63	4.77	28.56	15.16	13.86	5.22	30.17
Lower CI Нижняя граница ДИ	13.93	12.03	4.28	20.79	13.87	12.17	4.28	21.35
student t test t-критерий Стьюдента	0.97	0.75	0.42	0.73				

Clinoid triangle: Watanabe et al., reported measurements of 9.5, 13.3, 7.2 mm and 32.3 mm² (medial border, lateral border, base, and area) [4]. Isolan et al., reported measurements of 7.34, 13.89, 8.53 mm and 26.25 mm² (medial border, lateral border, base, and area) [23]. Day and Fukushima reported measurements of 6.30, 6.88 and 8.72 mm (medial border, lateral border and base) [24]. The findings of our study (7.64, 14.5, 8.69 mm and 26.02 mm² medial border, lateral border, base and area respectively) are in line with the Watanabe and Isolan studies.

Oculomotor triangle: This triangle is important during oculomotor nerve exposure and in cases of aneurysm of ICA at the crossing of posterior communicating artery with ICA. The average measurements are 10.4, 16.1, 12.2 mm (anterior, posterior and medial respectively). There is a discrepancy in describing the extent of the triangle. Day et al have defined triangle with subclinoid carotid segment, posterior clinoid process and porus oculomotorius. They have specifically named it as medial triangle [24]. This resulted in differences in dimensions as well. Umansky reported a measurements of 9.6, 16.6, 13.8 mm (anterior, posterior and medial respectively) [25]. Our results are in line with Umansky study outcomes.

Supratrochlear triangle: Wantabee reports dimensions of 10.9, 14.0, and 7.0 mm for medial, lateral and base measurements of this triangle [4]. Whereas, Doniel et al. reports measurement of 13.18, 14.27, and 5.51 mm respectively [12]. Results of this study (10.81, 14.94, 5.51 mm for medial, lateral and base) are similar to both these studies. During transcavernous approach, supratrochlear triangle is exposed to find the carotid-oculomotor membrane, distal dural ring (Figure 2), and meningo-hypophyseal trunk.

Infratrochlear triangle: Harris et al in their cadaveric study, reported an average length of 13 mm (medial border), 14 mm (lateral border) and 6 mm (base) respectively [26]. They report that this space can be enlarged by displacing the ophthalmic nerve and trochlear nerve. Few authors have called inferior trochlear triangle as lateral triangle [4, 18]. There is discrepancy in naming the triangle, a uniform definition of the triangle avoids confusion. Defining the borders and contents of the triangle provides better understanding of the superior quadrangular area.

Conclusion

Morphometric measurements of parasellar middle cranial fossa triangles, namely, clinoid triangle, oculomotor triangle, supratrochlear and infratrochlear triangle are presented.

REFERENCES

1. Emanuelli E, Zanotti C, Munari S, Baldovin M, Schiavo G, Denaro L. Sellar and parasellar lesions: multidisciplinary management. *Acta Otorhinolaryngol Ital.* 2021 Apr;41(2 Suppl 1):S30–41.
2. Komatsu F, Oda S, Shimoda M, Imai M, Shigematsu H, Komatsu M, et al. Endoscopic Endonasal Approach to the Middle Cranial Fossa through the Cavernous Sinus Triangles: Anatomical Considerations. *Neurol Med Chir (Tokyo).* 2014 Dec;54(12):1004–8.
3. Almeida JP, de Andrade E, Reghin-Neto M, Radovanovic I, Recinos PF, Kshetry VR. From Above and Below: The Microsurgical Anatomy of Endoscopic Endonasal and Transcranial Microsurgical Approaches to the Parasellar Region. *World Neurosurgery.* 2022 Mar 1; 159:e139–60.
4. Watanabe A, Nagaseki Y, Ohkubo S, Ohhashi Y, Horikoshi T, Nishigaya K, et al. Anatomical variations of the ten triangles around the cavernous sinus. *Clin Anat.* 2003 Jan;16(1):9–14.
5. Dagtekin A, Avci E, Uzmansel D, Kurtoglu Z, Kara E, Uluc K, et al. Microsurgical anatomy and variations of the anterior clinoid process. *Turk Neurosurg.* 2014;24(4):484–93.
6. Mathkour M, Werner C, Berry JF, Wysiadecki G, Walocha J, Iwanaga J, et al. Hakuba's triangle: a cadaveric study detailing its anatomy and neurovascular contents with vascular and skull base implications. *Neurosurg Rev.* 2022 Jun;45(3):2087–93.
7. Tayebi Meybodi A, Gandhi S, Mascitelli J, Bozkurt B, Bot G, Preul MC, et al. The oculomotor-tentorial triangle. Part I: microsurgical anatomy and techniques to enhance exposure. *J Neurosurg.* 2018 Jun 1;1–9.
8. Park HK, Rha HK, Lee KJ, Chough CK, Joo W. Microsurgical Anatomy of the Oculomotor Nerve. *Clinical Anatomy.* 2017;30(1):21–31.
9. Xu Y, Nunez MA, Mohyeldin A, Vigo V, Mao Y, Cohen-Gadol AA, et al. Microsurgical anatomy of the dorsal clinoid space: implications for

- endoscopic endonasal parasellar surgery. *Journal of Neurosurgery*. 2022 Feb 4;137(5):1418–30.
10. Volovici V, Varvari I, Dirven CMF, Dammers R. The membrane of Lilliequist—a safe haven in the middle of the brain. A narrative review. *Acta Neurochir*. 2020 Sep 1;162(9):2235–44.
 11. Benner D, Hendricks BK, Benet A, Graffeo CS, Scherschinski L, Srinivasan VM, et al. A system of anatomical triangles defining dissection routes to brainstem cavernous malformations: definitions and application to a cohort of 183 patients. *Journal of Neurosurgery*. 2022 Aug 26;1(aop):1–17.
 12. Drazin D, Wang JM, Alonso F, Patel DM, Granger A, Shoja MM, et al. Intracranial Anatomical Triangles: A Comprehensive Illustrated Review. *Cureus [Internet]*. [cited 2020 Aug 23];9(10). Available from: <https://www.ncbi.nlm.nih.gov/pmc/articles/PMC5714398/>
 13. Hendricks BK, Benet A, Lawrence PM, Benner D, Preul MC, Lawton MT. Anatomical Triangles for Use in Skull Base Surgery: A Comprehensive Review. *World Neurosurgery*. 2022 Aug 1;164:79–92.
 14. Kına H, Ayran A, Demirtaş İ. Microsurgical anatomy of the cavernous sinus and limitations of surgical approaches: a cadaveric study. *Folia Morphol (Warsz)*. 2022 Dec 27.
 15. Dolenc VV. *Microsurgical Anatomy and Surgery of the Central Skull Base [Internet]*. Wien: Springer-Verlag; 2003 [cited 2020 Nov 10]. Available from: <https://www.springer.com/gp/book/9783211832363>
 16. Parkinson D. A surgical approach to the cavernous portion of the carotid artery. *Anatomical studies and case report. J Neurosurg*. 1965 Nov;23(5):474–83.
 17. Parkinson D. Collateral circulation of cavernous carotid artery: anatomy. *Can J Surg*. 1964 Jul;7:251–68.
 18. Day JD, Tschabitscher M, Matula C. *Microsurgical dissection of the cranial base*. New York: Churchill Livingstone; 1996.
 19. Weisstein EW. Heron's Formula [Internet]. Wolfram Research, Inc.; [cited 2023 Jan 1]. Available from: <https://mathworld.wolfram.com/>
 20. Janakiram N, Sethi DS, Sharma SB, editors. *Atlas of Sellar, Suprasellar, and Parasellar Lesions [Internet]*. 1st ed. Noida: Thieme Medical and Scientific Publishers Private Limited.; 2020 [cited 2023 Jan 1]. Available from: <http://www.thieme-connect.de/DOI/DOI?10.1055/b000000680>
 21. Jung IH, Yoo J, Choi S, Lim SH, Ko J, Roh TH, et al. Endoscopic transorbital approach to the cavernous sinus: Cadaveric anatomy study and clinical application (SevEN-009). *Front Oncol*. 2022 Aug 26;12:962598.
 22. Kassam AB, Prevedello DM, Carrau RL, Snyderman CH, Gardner P, Osawa S, et al. The front door to meckel's cave: an anteromedial corridor via expanded endoscopic endonasal approach—technical considerations and clinical series. *Neurosurgery*. 2009 Mar;64(3 Suppl):ons71–82; discussion ons82–83.
 23. Isolan GR, Krayenbühl N, de Oliveira E, Al-Mefty O. Microsurgical Anatomy of the Cavernous Sinus: Measurements of the Triangles in and around It. *Skull Base*. 2007 Nov;17(6):357–67.
 24. Day JD, Fukushima T, Giannotta SL. Innovations in surgical approach: lateral cranial base approaches. *Clin Neurosurg*. 1996;43:72–90.
 25. Umansky F, Valarezo A, Elidan J. The superior wall of the cavernous sinus: a microanatomical study. *J Neurosurg*. 1994 Dec;81(6):914–20.
 26. Harris FS, Rhoton AL. Anatomy of the cavernous sinus. A microsurgical study. *J Neurosurg*. 1976 Aug;45(2):169–80.

Поступила 22.01.2023

Получены положительные рецензии 12.07.23

Принята в печать 05.10.23

Received 22.01.2023

Positive reviews received 12.07.23

Accepted 05.10.23

Information about the authors:

Bollavaram Pullanna — PhD scholar, Yenepoya University, Mangalore, Karnataka, India

<https://orcid.org/my-orcid?orcid=0000-0002-8328-8278>

Ramakrishna Avadhani — Professor, Department of Anatomy, Yenepoya University, Mangalore, Karnataka, India. <https://orcid.org/0000-0001-9523-689X>

Viveka S. — Professor, Anatomy content creator, Healiosmed Academy, Bangalore, Karnataka, India. <https://orcid.org/0000-0001-7719-4024>

Anoop Shastri — Assistant Professor, Department of Neurology, Shivananda Shastri, Super speciality hospital, shikaripura, Shivamogga, Karnataka, India

Информация об авторах:

Боллаварам Пулланна — аспирант, Университет Енепойя, Мангалур, Карнатака, Индия. <https://orcid.org/my-orcid?orcid=0000-0002-8328-8278>

Рамакришна Авадхани — профессор, кафедра анатомии, Университет Енепойя, Мангалур, Карнатака, Индия. <https://orcid.org/0000-0001-9523-689X>

Вивека С. — профессор, автор пособий по анатомии, Академия Хеалиосмед, Бангалор, Карнатака, Индия. <https://orcid.org/0000-0001-7719-4024>

Ануп Шастри — доцент, кафедра неврологии, специализированная больница имени Шивананды Шастри, Шикарипура, Шивамогга, Карнатака, Индия